APPLIED SCIENCES AND ENGINEERING

A 3D culture platform enables development of zinc-binding prodrugs for targeted proliferation of β cells

Kisuk Yang[1,2,3,4,5]*, Miseon Lee[6,7]*, Peter Anthony Jones[1,2,3]*, Sophie S. Liu[1,2], Angela Zhou[1,2], Jun Xu[1,2], Vedagopuram Sreekanth[6,7], Jamie L. Y. Wu[1,2], Lillian Vo[1,2], Eunjee A. Lee[1,2,3], Ramona Pop[8], Yuhan Lee[1,2,3], Bridget K. Wagner[6], Douglas A. Melton[8], Amit Choudhary[6,7,9,10†], Jeffrey M. Karp[1,2,3,4†]

Copyright © 2020 The Authors, some rights reserved; exclusive licensee American Association for the Advancement of Science. No claim to original U.S. Government Works. Distributed under a Creative Commons Attribution NonCommercial License 4.0 (CC BY-NC).

Advances in treating β cell loss include islet replacement therapies or increasing cell proliferation rate in type 1 and type 2 diabetes, respectively. We propose developing multiple proliferation-inducing prodrugs that target high concentration of zinc ions in β cells. Unfortunately, typical two-dimensional (2D) cell cultures do not mimic in vivo conditions, displaying a markedly lowered zinc content, while 3D culture systems are laborious and expensive. Therefore, we developed the Disque Platform (DP)—a high-fidelity culture system where stem cell–derived β cells are reaggregated into thin, 3D discs within 2D 96-well plates. We validated the DP against standard 2D and 3D cultures and interrogated our zinc-activated prodrugs, which release their cargo upon zinc chelation—so preferentially in β cells. Through developing a reliable screening platform that bridges the advantages of 2D and 3D culture systems, we identified an effective hit that exhibits 2.4-fold increase in β cell proliferation compared to harmine.

INTRODUCTION

Pancreatic β cell loss is a common pathological feature of diabetes (*1*), leading to a β cell deficiency and dysfunction in insulin production (*2*). There is currently no durable and effective treatment for β cell loss (*3*) as there are no progenitor cell populations to replenish lost β cells; thus, constant monitoring and insulin injections are mandatory for life. Recently, pluripotent stem cell–derived β cells (SC β cells) have emerged as a promising approach to benefit a wider patient population than existing whole pancreas or islet transplantations as a sustainable source of cell-replacement therapy (*4*–*7*). However, SC β cells have an extremely low proliferation capacity and thus there has been a great effort to screen and develop small molecules that can encourage β cell proliferation. Unfortunately, these small molecules generally are not specific for β cells and often cause unmitigated proliferation in other cells at the necessary concentrations, leading to cytotoxic and genotoxic side effects (*8*).

Because β cells have over a million-fold higher Zn(II) concentration (10 to 20 mM) in insulin vesicles compared to α cells (1 nM) (*9*, *10*) and other cell types (~400 pM), we reasoned that hydrolytic reactions catalyzed by an excess of Zn(II) (*11*, *12*) could be used to deliver active drugs to zinc-rich β cells. We herein designed a zinc-binding prodrug (ZnPD) that establishes a release control based on the chelation of zinc ions to provide a method for sustained and specific delivery of drugs to β cells. However, standard 2D cell-culture systems, typically used for the rapid compound screening, do not have Zn(II) levels equivalent to physiological conditions. Three-dimensional (3D) culture systems, alternatively, preserve the morphological and biological complexity of pancreatic niches and recapitulate the myriad cell-to-cell and cell-to-matrix interactions that are important for maintaining appropriate intracellular Zn(II) levels. Although 3D culture systems for β cells, such as spinner flasks [SFs; a type of single use bioreactors (SUBs)] and microfluidic devices do exist, these platforms lack the simplicity and throughput of conventional 2D culture methods (*13*–*16*) to screen multiple ZnPDs and find therapeutically relevant compounds.

As a result, we established a reliable screening and culture platform, termed the Disque Platform (DP). The DP can reaggregate SC β cells into a thin disc-shaped layer within conventional well plates, and it recapitulates the 3D environments essential for β cells. As a screening tool for our newly developed ZnPDs, it also bridges the simplicity and high-throughput capability of 2D screening methods. The DP was validated against both 2D and 3D culture systems. We then applied the DP to the development of ZnPDs based on harmine, a DYRK1A inhibitor, which was recently identified as able to induce human β cell proliferation (*17*), although with systemic cytotoxic and genotoxic effects at the necessary concentrations (*8*). Our harmine-based ZnPD system consists of a cleavable bond between harmine and a zinc chelator that results in an active form of harmine released only upon zinc chelation. We then combined our two developments using the DP to test harmine-based ZnPDs, verifying the results via a 3D-reconstructed culture system. With this process, we detected increased harmine activity through SC β cell proliferation (2.4-fold increase compared to harmine), higher targeting efficiency, and decreased toxicity compared to unmodified harmine. Overall, the DP provides a simple and rapid screening method similar to 2D culture while retaining the cellular environment of a 3D culture, indicating the requirement for screening systems that better mimic native cell environments. These results were also translated in human primary islets and a scaled-up production of SC β cells in SF.

[1]Department of Anesthesiology, Perioperative and Pain Medicine, Brigham and Women's Hospital, Harvard Medical School, Boston, MA 02115, USA. [2]Center for Nanomedicine, Harvard Stem Cell Institute, Brigham and Women's Hospital, Harvard Medical School, Boston, MA 02115, USA. [3]Harvard-MIT Division of Health Sciences and Technology, Cambridge, MA 02139, USA. [4]Proteomics Platform, Broad Institute of MIT and Harvard, Cambridge, MA 02142, USA. [5]David H. Koch Institute for Integrative Cancer Research, MIT, Cambridge, MA 02142, USA. [6]Chemical Biology and Therapeutics Science, Broad Institute of MIT and Harvard, Cambridge, MA 02142, USA. [7]Department of Medicine, Harvard Medical School, Boston, MA 02115, USA. [8]Department of Stem Cell and Regenerative Biology, Harvard Stem Cell Institute, Harvard University, Cambridge, MA 02138, USA. [9]Divisions of Renal Medicine and Engineering, Brigham and Women's Hospital, Boston, MA 02115, USA. [10]Chemical Biology Program, Harvard University, Cambridge, MA 02138, USA.
*These authors contributed equally to this work.
†Corresponding author. Email: jeffkarp@mit.edu (J.M.K.); achoudhary@bwh.harvard.edu (A.C.)

RESULTS

Design and optimization of the DP for screening ZnPD system

Initial experiments measuring the zinc content and junction proteins [E-cadherin (E-cad) and connexin 36 (CX36)] in SC β cells revealed significantly decreased gene expression and Zn(II) levels in 2D culture compared to 3D culture (SF) (fig. S1, see text S1). Because prodrugs use distinct physiological features in cells, this suggests that these 2D cultures that do not fully recapitulate 3D culture environments would not be sufficient for our designed experiments in screening prodrugs. As a result, we sought to establish a reliable screening and culture platform to bridge the simplicity and high-throughput capability of 2D culture methods and the 3D environments essential for mimicking the natural cellular makeup of β cells to effectively screen newly developed prodrugs (Fig. 1). In developing this platform, certain key features of 3D culture needed to be preserved in a 2D-type system: (i) the cell-cell and cell-matrix junctions, (ii) high cell viability during the study period, (iii) ability for cells to differentiate to fully functional β cell microtissues, and (iv) compatible with current readouts to assess the therapeutic effects of potential chemical factors.

We herein developed the DP which allows a rapid reaggregation of SC β clusters into flat 3D discs that can maximize surface area for oxygen and nutrient diffusion and be cultured in commercially available multi–well culture plates (Figs. 1 and 2A). SC β cell discs are formed in a "Disque," which refers to a laser-cut acrylic mold made up of a circular compartment containing the cell disc and a straight edge to accommodate multipipette tip placement that simplifies media changes and assays. A semipermeable hydrophilic polytetrafluoroethylene (PTFE) membrane with a 1.0-μm pore size was attached to the acrylic mold to support the cell discs. Furthermore, the semipermeable membrane was precoated with vasculature extracellular matrices (ECMs) (e.g., collagen IV and laminin), which are the main components of the basement membrane in developing human islets and are important for β cell survival, insulin secretion, architecture formation, and gene expression (*18*–*20*). In addition, to maintain media circulation and mitigate the generation of air bubbles, we elevated individual Disques by attaching a semicircular pedestal to the bottom. To form the cell discs, SC β clusters were dispersed into single cells, which were seeded into the individual Disques. The Disques were centrifuged to reform cell discs with controlled cell densities and dimensions in a regular flat-bottom 96-well plate (Fig. 2B). Cell discs grown using the ECM-coated DP promoted the gene expression of key pancreatic endoderm cell markers NK6 homeobox 1 (Nkx6.1) and pancreatic and duodenal homeobox 1 (Pdx-1) compared to the noncoated group (fig. S2), although there

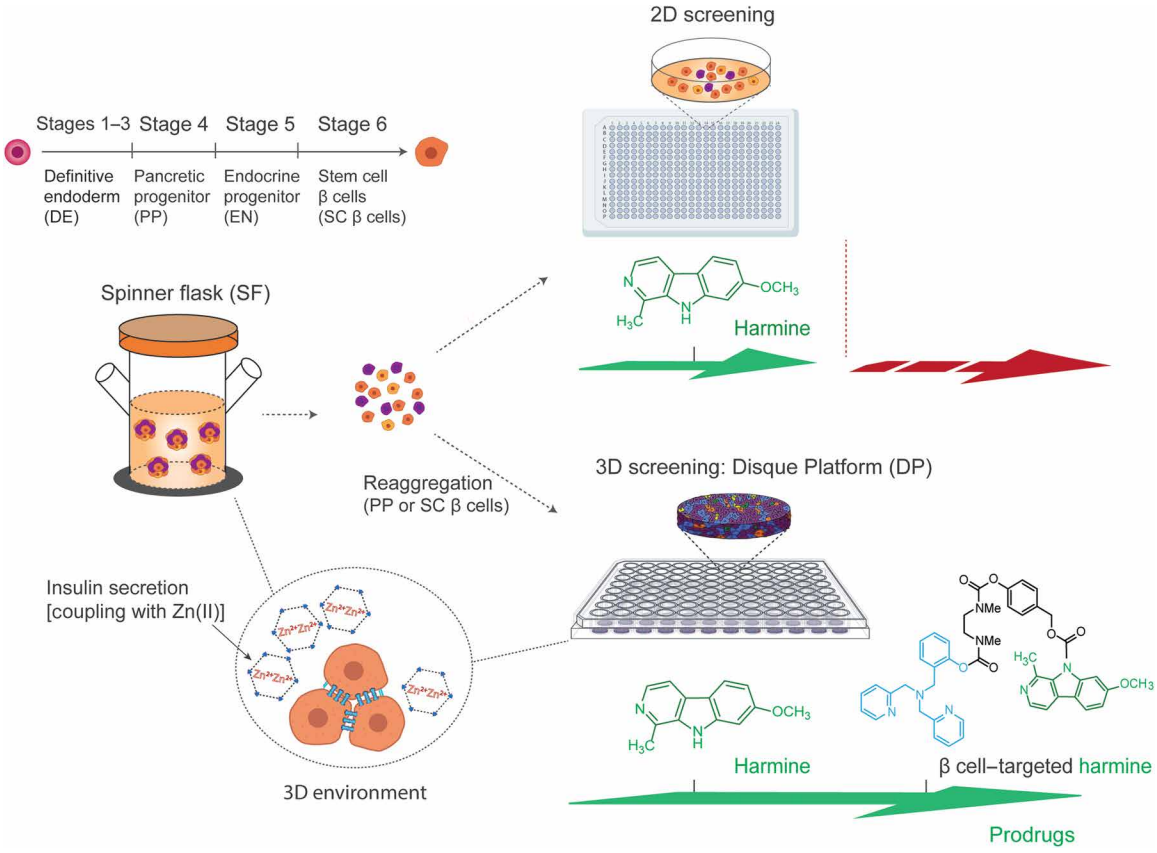

Fig. 1. The illustration demonstrates the need to establish a reliable platform that mimics the 3D environments essential for β cells to screen prodrugs (e.g., β cell–targeted harmine). Single use bioreactors (e.g., SF) are able to culture SC β cells and mimic native β cell environments, however, are not amenable to high-throughput screening. When screening β cell–targeted drugs, 2D screening platforms do not mimic in vivo conditions, especially cell-cell interactions, and zinc ion levels, which hinder reliable screening of prodrugs. Therefore, a 3D screening platform is needed for developing prodrugs that can mimic native β cell environments with the ability to accommodate 2D screening methods.

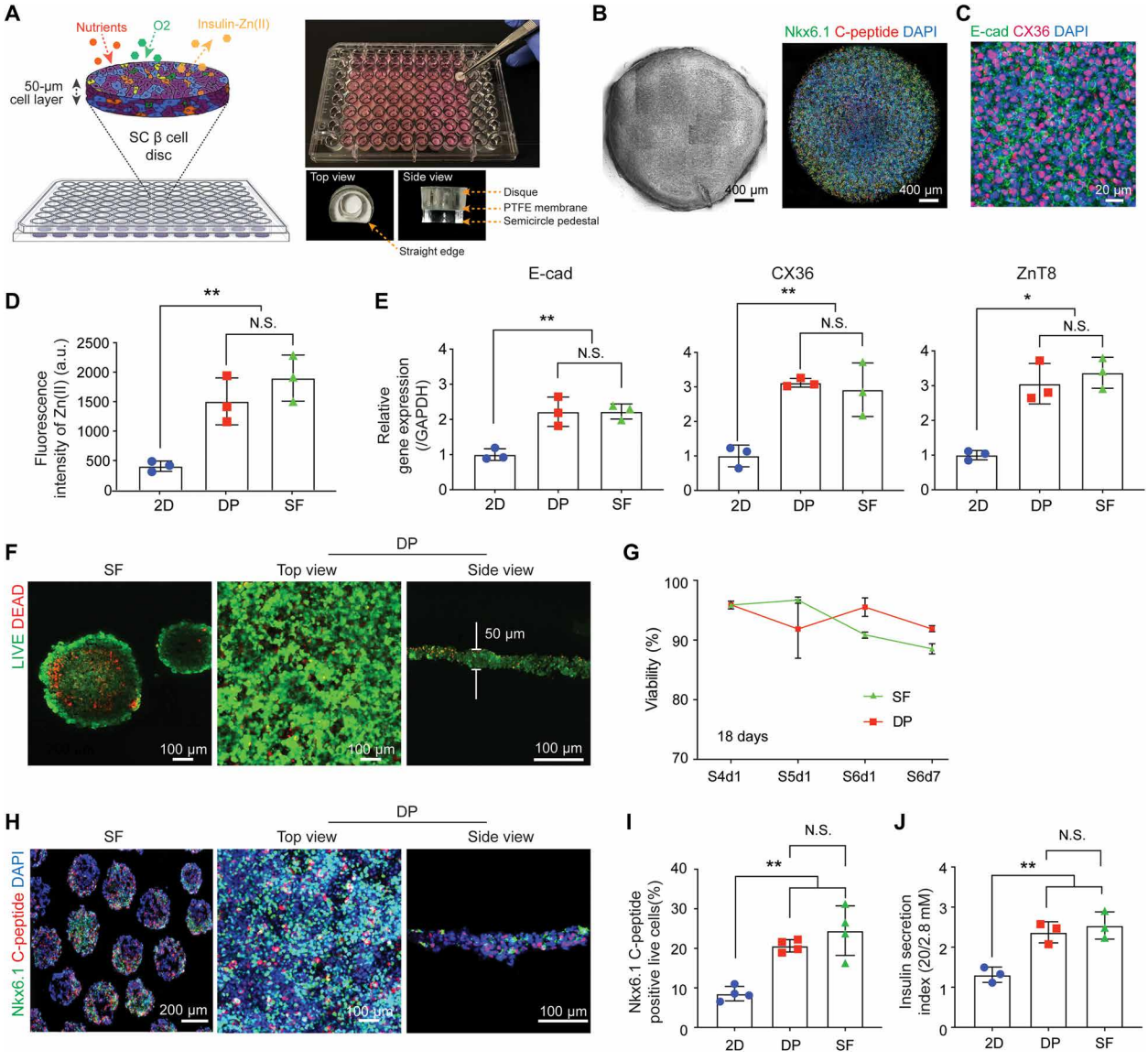

Fig. 2. Disque Platform. (**A**) Scheme and gross view of 3D reconstructed SC β cells in Disque Platform (DP). (**B**) Cell disc morphology shown through bright-field and confocal microscopy [NK6 homeobox 1 (Nkx6.1) and C-peptide]. (**C**) Immunofluorescent staining of E-cadherin (E-cad) and connexin 36 (CX36) in cell discs. (**D**) 3D cultures (DP and SF) showed significantly higher levels of Zn(II) compared to conventional 2D system (2D monolayer), measured through signal intensity from FluoZin-3 indicator dye ($n = 3$, $^{**}P < 0.01$ versus 2D). N.S., not significant; a.u., arbitrary units. (**E**) SC β cells cultured in DP show significantly higher gene expression of E-cad, CX36, and zinc transporter 8 (ZnT8) using quantitative real-time polymerase chain reaction analysis ($n = 3$, $^{*}P < 0.05$, $^{**}P < 0.01$ versus 2D). (**F**) Homogenous distribution of viable pancreatic progenitor (PP) cells in DP via LIVE/DEAD assay (5-day differentiation). (**G**) DP achieved high percentage of viable cells comparable to SF culture during PP differentiation to SC β cells [stage 4 day 1 (S4d1) to S6d7)] via flow cytometry analysis with the Zombie Aqua Fixable Viability Kit ($n = 3$). (**H**) DP shows similar expression of C-peptide and Nkx6.1 in SC β cells to SF through immunocytochemistry staining and (**I**) flow cytometry analysis ($n = 4$, $^{**}P < 0.01$ versus 2D). (**J**) SC β cells show similar glucose stimulated insulin secretion index between DP and SF ($n = 3$, $^{**}P < 0.01$ versus 2D).

were no significant differences between the gene expression of both markers in 2D culture conditions. On the basis of these experimental data (fig. S3, see text S2), we established the following parameters for the DP: The thickness was set to 50 μm, and the diameter was set to 3000 μm for ease of operation (e.g., during cell seeding and Disque replacement).

Validation of DP for effective SC β cell culture and drug screening

After optimizing the DP, we evaluated its ability to support the viability, differentiation, and function of cell discs compared to dissociated SC β cells in 2D monolayer culture and 3D SC β clusters cultured from SFs, the current gold-standard suspension flask culture system. We hypothesized that the DP could promote direct contact between SC β cells and the formation of 3D microtissue with cell-cell junctions, which can better direct the course of β cell differentiation and Zn(II) levels compared to dispersed cells in 2D (*21*). Immunofluorescent imaging showed that the cell discs successfully reestablished cell-cell interactions (E-cad and CX36) among the homogenously distributed and densely packed SC β cells (Fig. 2C). We were next interested in whether the Zn(II) concentration was reflected in the

increased junction markers, as cell-cell contacts are important for zinc signaling (*11*, *12*), in DP and SF compared to 2D culture. Gene expression levels of E-cad, CX36, and zinc transporter 8 (ZnT8) from quantitative real-time polymerase chain reaction (qRT-PCR) and the intracellular Zn(II) level from DP-cultured cells were similar to 3D SC β clusters from SF. In contrast, 2D culture showed significantly lower levels of the junction markers and Zn(II) (Fig. 2, D and E).

Next, we hypothesized that the optimized cell culture parameters would maintain a high cell viability despite occurring in static 3D culture (DP) rather than suspension culture during differentiation. The DP achieved a comparable high viability to SF culture during pancreatic progenitor (PP) (stage 4, S4) differentiation to SC β cells (stage 6, S6) (Fig. 2, F and G). To validate the DP's efficacy in supporting SC β cell viability and differentiation, we collected PP cells from the same biological batch and cultured them in parallel in DP and SF with the same differentiation protocol from the PP cells to SC β cells (*22*). After 5 days in culture, the confocal microscopy of the cell discs revealed a uniform distribution of live cells (Fig. 2F). Following 18 days of differentiation, we observed a comparable viability profile between DP and SF and similar levels of coexpression of β cell markers C-peptide (a component of proinsulin) (*23*) and Nkx6.1, which suggest that the DP can be used for long-term culture (Fig. 2, H and I).

Next, we further examined whether other junction signaling pathways critical for β cell differentiation, such as the Notch signaling pathway, could be supported in the DP, as Notch inhibition in PP cells is known to promote differentiation into the endocrine lineage and β cell production (*24*, *25*). To measure this in the DP, we supplemented the differentiation protocol of PP cells with Notch inhibitor [γ-secretase inhibitor, *N*-[*N*-(3,5-difluorophenacetyl)-L-alanyl]-S-phenylglycine t-butyl ester (DAPT) (10 μM)] and examined the cells at the end of PP cells [stage 4 day 5 (S4d5)] by immunocytochemistry and gene expression analysis (fig. S4). Immunocytochemical staining for Pdx-1 and Nkx6.1 showed that the copositive progenitor cells, which do not continue to differentiate to endocrine progenitors due to Notch signaling (*26*), were significantly increased after Notch inhibition (fig. S4, A and B). Meanwhile, gene expression results from cells cultured in the DP showed a 1.9-fold increase in Pdx-1 expression, 1.5-fold increase in Neurogenin3, which are consistent with downstream effects of Notch inhibition in pancreatic lineage differentiation. Furthermore, as expected, Notch inhibition lead to a 0.4-fold decrease in SOX9 which maintains PP cells (*27*) and a 0.2-fold decrease in hairy and enhancer of split1 (Hes1) expression, which is an essential downstream effector of Notch signaling predominantly expressed by pancreatic cells (fig. S4, C and D) (*25*, *28*). The Hes1 expression in 2D culture was not responsive to lateral Notch inhibition (fig. S4D). Together, these data indicated that the cells could be maintained and differentiated from PP cells to SC β cells in the DP, and that there is a difference in the ability to recapitulate Notch inhibition between 2D- and 3D-like culture systems. Upon establishing the differentiation capabilities of the DP, we then reasoned whether differentiated SC β cells also elicited proper insulin secretion functionality. The DP also supported insulin secretion from SC β cells in response to glucose stimulation, and similar secretion indices were noted between DP and SF (Fig. 2J).

Zinc-binding scaffold for β cell–specific delivery of harmine

Harmine, a DYRK1A inhibitor, has recently been found as an effective agent for β cell proliferation; however, numerous reports have also identified it as an effective antitumor agent at high concentrations due to its ability to intercalate DNA and induce apoptosis (*8*, *29*, *30*). Consequently, this limits the therapeutic range of concentrations that can be used for β cell proliferation. Furthermore, harmine analogs also highly induce proliferation of α cells as well as other endocrine cell populations, which further limits the efficacy of harmine for β cell regeneration in diabetes (*31*–*33*). Thus, to use harmine as an agent specific for β cell proliferation, a fine balance between maximizing dosage for obtaining robust proliferation responses and avoiding cytotoxic effects needs to be achieved.

Therefore, we created a harmine-based ZnPD that would specifically target β cells. The ZnPD consisted of three components: an inactive form of harmine, a Zn(II)-binding ligand, and a self-immolative linker that linked these two components. Upon Zn(II) binding, the carbamate linkage hydrolyzes and triggers self-immolation to release an active harmine (Fig. 3A). Using boron-dipyrromethene (BODIPY) acid as a fluorescent cargo conjugated to the zinc-binding scaffold, we synthesized ZnPD4 (Fig. 3B) to visualize the unmasking of fluorescent cargo in SC β cells. The carbamate linkage was cleaved upon Zn(II) binding, and selective fluorophore emission was observed in SC β cells in a dose-dependent manner (Fig. 3B). Previously, we and other groups also characterized zinc-chelating ligands for imaging and proliferation purposes and reported the kinetics of zinc-catalyzed hydrolysis in multiple ZnPD systems, both biochemically and in β cells (*34*). In all of these systems, kinetics of release of our ZnPDs were monitored and release was shown to occur within one hour in β cells, similar to what has been reported by Lippard and co-workers (*35*).

As a control, fluorescence was not emitted in PP cells, which do not participate in insulin production and, therefore, have lower Zn(II) concentration (fig. S5A) (*36*). To mimic in vivo Zn(II) levels, we pretreated cells with 50 μM zinc chloride (*37*). Pretreating SC β cells with zinc chloride did not modify the ZnPD targeting, suggesting that β cell zinc homeostasis was highly regulated (fig. S5, A and B). Using SC β cells, unmasked ZnPD4 signal more closely matched the distribution of C-peptide$^+$ SC β cells than glucagon (GCG) stained cells (Fig. 3C and fig. S6). Because C-peptide is a polypeptide cleaved off from proinsulin and packaged along with insulin into the secretory granules, this distribution profile strongly suggested that ZnPD targeted the Zn(II)-rich secretory granules in β cells and not the PP cells that do not produce insulin. Furthermore, previous literature, which has reported colocalization of Zn(II) and insulin, supports the punctate patterning of ZnPD4, suggesting that zinc chelation and BODIPY release occur in specific patterns of the insulin granules (*38*). In addition, flow cytometry data also revealed that the ZnPD system was more selective toward C-peptide–producing cells by over threefold compared to non–C-peptide$^+$ cells (e.g., α cells, δ cells, pancreatic polypeptide cells) (Fig. 3D). Overall, these data implied that the ZnPD could reduce its off-target activity in non–β cell lines or other subpopulations of the pancreatic endocrine lineage and help target the therapeutic effect of small-molecule inducers to the insulin-producing SC β cells.

Screening and validation of ZnPDs in DP

We were first interested in determining candidates that were suitable for driving PP cell population for further expansion. Accordingly, to synthesize prodrugs (ZnPDs) (table S1), we screened multiple parent small molecules in both PP and SC β cells and found that harmine emerged as the most efficacious for driving PP cells toward further differentiation of SC β cells (fig. S7, A and B). In addition,

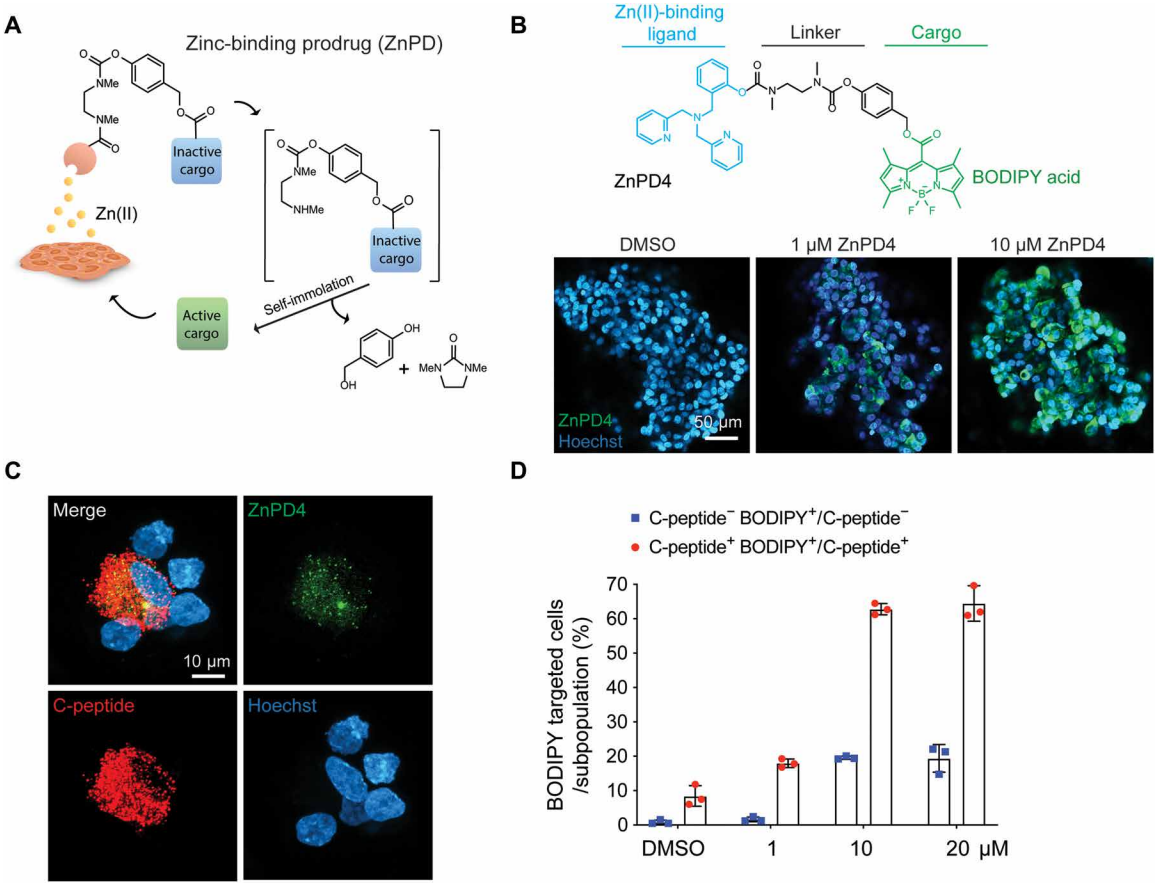

Fig. 3. A ZnPD system is developed to enable intracellular exposure of drug targeting β cells. (**A**) Scheme of the ZnPD system: ZnPD comprises a zinc chelating group, a linker, and an inactive cargo. Zn(II) selectively catalyzes the bond cleavage and release the active form of a drug in β cells. This ZnPD system completely releases the active cargo as the carbamate linkage hydrolyzes and triggers self-immolation. (**B**) A fluorescent dye, boron-dipyrromethene (BODIPY) acid, is used as the first cargo to visually confirm that the drug releases in SC β cells. Representative images show the dose-dependent ZnPD4 unmasking in SC β cells cultured in SF and nuclear staining (Hoechst). (**C**) Fluorescent signal from activated ZnPD4 is selective in SC β cells cultured in SF as shown through confocal images. (**D**) ZnPD system is more selective toward C-peptide$^+$ cells, compared to C-peptide$^-$ cells (e.g., α cells, δ cells, and polypeptide cells), measured by BODIPY fluorescence signal through flow cytometry ($n = 3$).

we tested harmine analog, AnnH79 that does not inhibit DYRK1A and used it as a negative control (*39*). Assessing the population of proliferating monohormonal SC β cells by flow cytometry revealed a statistically significant increase with harmine compared to the dimethyl sulfoxide (DMSO) control or negative control (fig. S7C). This data indicated that the DP can reliably replicate β cell niches and can identify a known β cell–proliferating small-molecule inducer (harmine). Next, we synthesized several ZnPDs that contained harmine as the active cargo (ZnPD6–8), with ZnPD8 acting as the negative control because it contained a noncleavable linker that could not release harmine as a cargo (Fig. 4A and fig. S8). We then compared the ZnPDs and harmine over the range of 0.625 to 20 μM, in twofold increases. On the basis of the percentage of proliferating SC β cells using the C-peptide and EdU copositive metric, wherein EdU is a proliferation marker that identifies cells undergoing DNA replication in the *S* phase. We successfully identified ZnPD6 as the best hits based on the coexpression of C-peptide and EdU in SC β cells [analyzed with one-way analysis of variance (ANOVA)] (Fig. 4B). We also noticed an increase in C-peptide and EdU copositive cell population for both concentrations of ZnPD6 (3.4-fold and 3.1-fold versus DMSO, 20 μM and 10 μM) (DMSO: 0.82%; ZnPD6 20 μM: 2.79%; ZnPD6 10 μM: 2.56%) but not in the ZnPD8 control (ZnPD8 20 μM: 0.31%; ZnPD8 10 μM: 0.28%) (Fig. 4B). However, no difference was observed between 10 and 20 μM ZnPD6 in C-peptide and EdU copositive cell population. Thus, to investigate the targeting efficiency of ZnPD6, we also examined C-peptide$^+$ GCG$^-$ EdU$^+$ cell population using flow cytometry, which was significantly increased for ZnPD6 at 20 μM compared to 10 μM (fig. S9). There was no significant difference between the no treatment and DMSO group. The cytotoxicity curve revealed that harmine had a cytotoxic effect over 10 μM, and a similar trend was observed in ZnPD7, while ZnPD6 elicited cytotoxicity only at higher doses (Fig. 4C). Accordingly, we selected ZnPD6 over ZnPD7 for further examination because ZnPD6 induces higher propensity of copositive cells (C-peptide and EdU) and can potentially be used at higher doses than nonmodified harmine.

Despite releasing the same drug following ZnPD cleavage, we were interested in determining what caused the difference in cytotoxicity and proliferation between ZnPD6 and unmodified harmine. We, therefore, examined harmine and ZnPD6 at their optimal concentrations for proliferation, 10 and 20 μM, respectively. Following 6 days of culture with drug treatments every 3 days, ZnPD6 exhibited a

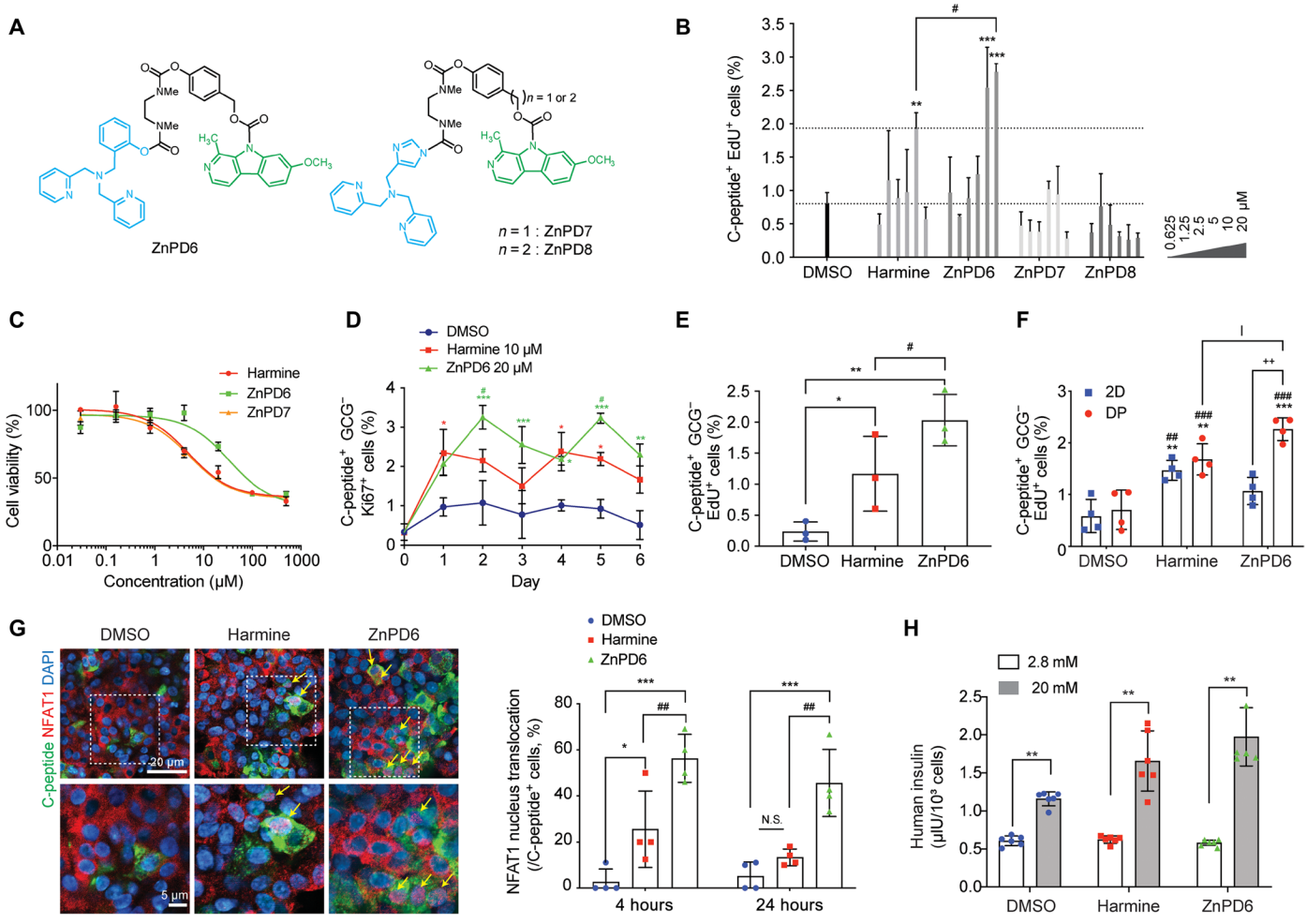

Fig. 4. Testing ZnPDs in DP reveals ZnPD6 as a targeted β cell proliferation inducer. (**A**) Structure of harmine conjugated ZnPDs. (**B**) SC β cells treated in DP successfully identified ZnPD6 as a candidate for increasing β cell proliferation via flow cytometry ($n = 3$, $^{**}P < 0.01$, $^{***}P < 0.001$ versus DMSO, $\#P < 0.05$ versus harmine). (**C**) Cell viability of SC β cells is measured by alamarBlue assay (0.032 to 500 μM, $n = 3$). (**D**) ZnPD6 exhibits increased and prolonged proliferation profile of SC β cells compared to harmine and DMSO over 6-day treatment ($n = 3$, $^{*}P < 0.05$, $^{**}P < 0.01$, $^{***}P < 0.001$ versus DMSO, $\#P < 0.05$ versus harmine). (**E**) Treatment of ZnPD6 to human primary islets in DP reveals higher inductive effect compared to DMSO and harmine ($n = 3$, $^{*}P < 0.05$, $^{**}P < 0.01$ versus DMSO, $\#P < 0.05$ versus harmine). (**F**) ZnPD6 in the DP induces a higher increase in the population of proliferating SC β cells compared to DMSO and harmine [$n = 4$, $^{**}P < 0.01$, $^{***}P < 0.001$ versus DMSO (DP), $\#\#P < 0.01$, $\#\#\#P < 0.001$ versus DMSO (2D), $|P < 0.05$ versus harmine (DP), $++P < 0.01$ versus ZnPD6 (2D)]. (**G**) Increased NFAT1 nuclear translocation with ZnPD6 versus harmine in SC β cells (magnified images below). Yellow arrows indicate copositive C-peptide and nuclear NFAT1 cells. ZnPD6 sustains NFAT1 nuclear translocation at 24 hours versus harmine ($n = 4$, $^{*}P < 0.05$, $^{***}P < 0.001$ versus DMSO, $\#\#P < 0.01$ versus harmine) in the DP. (**H**) Insulin secretion of SC β cells subject to glucose stimulation ($n = 5$ to 6, $^{**}P < 0.01$ versus 2.8 mM).

delayed but enhanced β cell proliferation (C-peptide$^+$ GCG$^-$ Ki67$^+$) response (Fig. 4D). This data suggest that the attenuated cytotoxicity with ZnPD6 may be due to a decrease in the initial burst of harmine and a prolonged local concentration of harmine delivered to cells through a delayed release. Two treatments of ZnPD6 to human primary islets in DP also revealed β cell proliferation, and the inductive effect of ZnPD6 at 20 μM showed an 8.7-fold increase compared to the control and a 2.4-fold increase compared to harmine (10 μM) (Fig. 4E). ZnPD6 induced a greater increase in the population of proliferating β cells, 3.2-fold compared to DMSO and 1.3-fold compared to harmine, in the DP, while in a conventional 2D system, ZnPD6 did not show any significant differences in proliferation compared to DMSO (Fig. 4F), indicating the importance of screening compounds in a system that mimics the 3D in vivo cellular environment.

To confirm whether ZnPD6 could prolong the drug response, we used nuclear factor of activated T cells 1 (NFAT1) protein nuclear translocation as a readout for DYRK1A inhibition, which was found to be maintained for up to 4 hours (*40*). We hypothesized that ZnPD6 could prolong the duration of NFAT1 nuclear translocation to cause sustained proliferation versus unmodified harmine due to the cleavage delay. We found that NFAT1 translocation of SC β cells was sustained for up to 24 hours with ZnPD6 treatment, while NFAT1 nuclear translocation decreased from 25.6 to 13.4% at 24 hours with harmine treatment (Fig. 4G). In addition, ZnPD6 shows higher targeting efficiency, reflected by NFAT1 translocation in C-peptide$^+$ β cells, such that a higher dose can be delivered to SC β cells to enhance NFAT1 translocation. Therefore, ZnPD6 demonstrates a sustained action and greater targeting efficiency for C-peptide$^+$ cells. Last, insulin secretion from SC β cells treated with ZnPD6 in

the DP was also appropriately responsive to glucose stimulation (Fig. 4H).

Examination of ZnPD6 in SF

We then validated whether the hit obtained from the DP could elicit similar effects for SC β cells in a SUB that is commonly used in clinical scale-up. Therefore, we tested the efficacy of ZnPD6 in an SF to validate its potential at inducing proliferation and differentiation of SC β clusters for clinical translation (Fig. 5A). After treatment with ZnPD6, reconstructed confocal images showed an increased propensity for cells copositive for C-peptide and EdU, which are marked by white arrows in the representative images (Fig. 5B). It is well known that, at the terminal stage of SC β cell differentiation, there is still a large population of polyhormonal cells, so the population of proliferating monohormonal β cells (C-peptide$^+$ GCG$^-$) was also examined, and we observed a 2.8-fold higher EdU incorporation in the ZnPD6-treated group compared to the control and 1.3-fold higher compared to harmine. There was no significant difference in proliferation between ZnPD6 and DMSO in α cells, indicating a selective release of harmine in β cells but not α cells (C-peptide$^-$ GCG$^+$) (Fig. 5C). ZnPD6 treatment also showed an increase in Nkx6.1 and insulin gene expression compared to untreated control and harmine (Fig. 5D), suggesting a potential increase in functional insulin secretion. Accordingly, we performed a glucose stimulated insulin secretion index (GSIS) test and revealed that upon glucose stimulation, SC β cells insulin secretion increased after compound treatment (Fig. 5E), with a GSIS index of 3.39 in DP, similar to 3.05 in SF. The insulin secretion from SC β cells treated with ZnPD6 in both DP and SF was also appropriately responsive to glucose stimulation suggesting that ZnPD6 treatment did not majorly affect insulin secretion or packaging capabilities. Overall, the results indicate that ZnPD6 is an effective molecule for enhancing proliferation and targeting, and that it maintains comparable functional performance when tested in both SF and DP.

DISCUSSION

Our focus on developing a ZnPD for targeting β cells led to the need for culture systems that better mimicked in vivo conditions than currently existing 2D culture systems in a more high-throughput

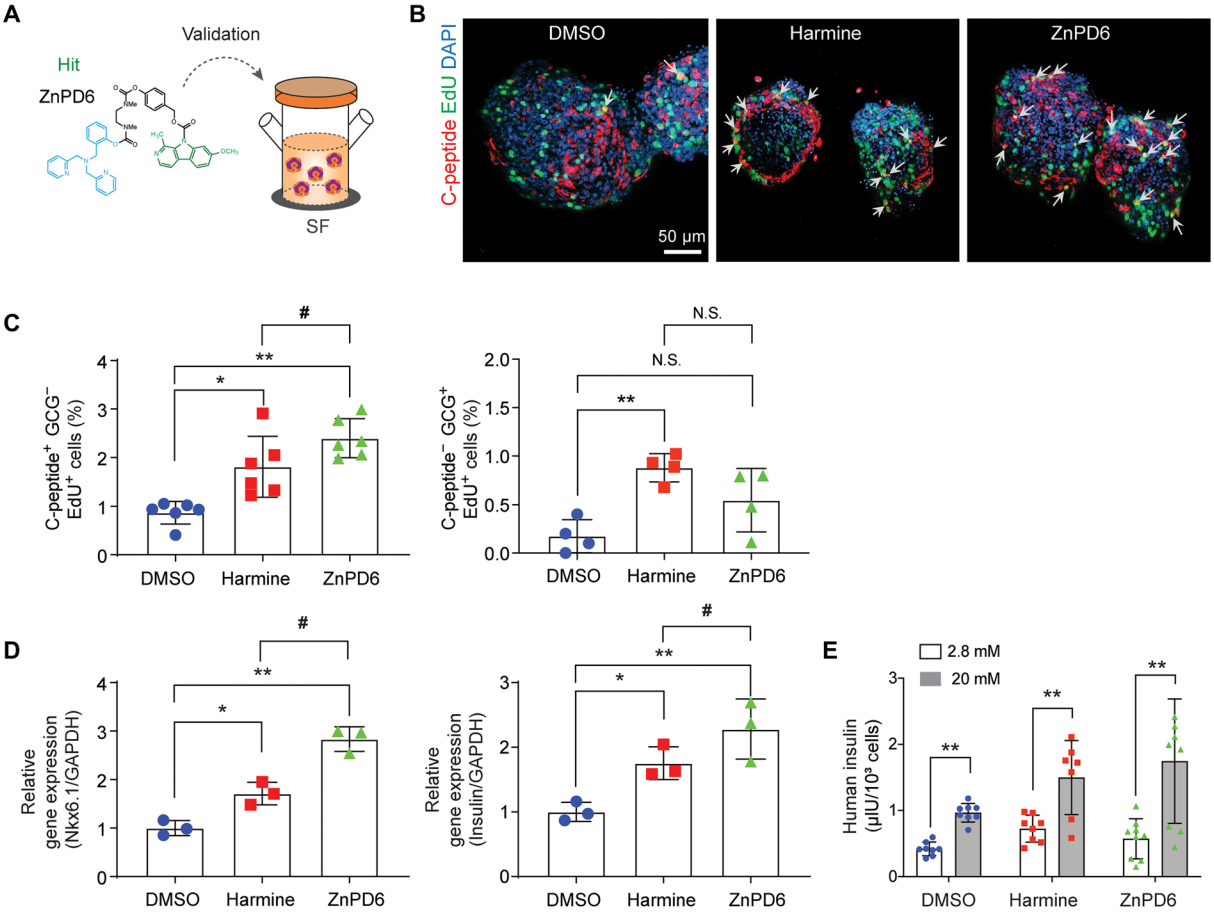

Fig. 5. SC β cell proliferation and differentiation capacity of ZnPD6 are validated in a SF. ZnPD6 shows higher efficacy than unmodified harmine in a scaled-up culture of SC β cells. (**A**) ZnPD6 identified from the DP is validated in SF for scaled-up SC β cell culture. (**B**) Treatment with ZnPD6 increases propensity of C-peptide and EdU copositive SC β cells as seen through representative immunofluorescent images of SC β cells with C-peptide (red), EdU (green), and nuclear staining (DAPI). White arrows indicate coincident cells (yellow). (**C**) EdU incorporation in monohormonal β cells treated with ZnPD6 is significantly higher compared to DMSO and harmine. Population of SC β cells (C-peptide$^+$ GCG$^-$ EdU$^+$) and SC α cells (C-peptide$^-$ GCG$^+$ EdU$^+$) treated in SF is obtained using flow cytometry ($n = 4$ or 6, $^*P < 0.05$, $^{**}P < 0.01$ versus DMSO, $\#P < 0.05$ versus harmine). (**D**) ZnPD6 treatment in SF increases Nkx6.1 and insulin gene expression compared to DMSO and harmine group ($n = 3$, $^*P < 0.05$, $^{**}P < 0.01$ versus DMSO, $\#P < 0.05$ versus harmine). (**E**) Insulin secretion in response to glucose stimulation ($n = 7$ to 9, $^{**}P < 0.01$ versus 2.8 mM).

fashion than the 3D suspension culture system. We, therefore, designed the DP to bridge the gap between the 2D and 3D culture platforms to permit a reliable, medium- to high-throughput, screening platform for β cells. We validated our system against current 2D and 3D culture systems and used it in a biologically relevant application—demonstrating that our harmine-based ZnPDs did selectively target β cells and increase β cell proliferation.

Human pancreatic islets comprise intricate multicellular compositions, and many of their attributes are retained only when the cells remain as components of the islet. Once β cells have been dissociated for 2D culture, their functions and activity have been observed to differ from islets, as we showed through their lower levels of junction markers and Zn(II), poor differentiation profiles, and less pronounced insulin secretion compared to 3D cultures. A key result from our DP method was that reaggregated SC β cell discs cultured in the DP were able to reestablish 3D microenvironments inside conventional 96-well plates. As a result, cell-cell and cell-ECM interactions were reestablished at levels similar to SC β clusters cultured in 3D suspension cultures, recapitulating the viability, differentiation capacity, and function of the 3D gold standard. Moreover, cell discs in the DP can be cultured over multiple stages of differentiation, suggesting the potential for long-term culture and drug screening study. Ultimately, the multiarray construction of the DP is entirely compatible with small-molecule screening strategies and mainstream assays [e.g., immunofluorescent imaging, enzyme-linked immunosorbent assay (ELISA), qRT-PCR, and flow cytometry]. These findings make the DP an attractive technology for performing drug screening with β cells with the convenience and throughput of current 2D culture methods while retaining the critical properties of the more cumbersome 3D methods. Further exploration to screen multiple factors at various stages of the differentiation pathway from PP to SC β cells in the DP is beneficial.

As opposed to 2D environments, the DP allowed for cells to be cultured with greater resemblance to that of a native islet environment with increased junction markers and Zn(II) concentration, therefore presenting a platform capable of interrogating the effects of different ZnPDs. With the ZnPD system, we successfully appended a zinc-chelating probe onto harmine to act as a controlled release mechanism that is activated in the Zn(II)-rich insulin vesicles, and we validated its function and selectivity using the DP. Functional studies revealed that the harmine-based ZnPD6 could induce proliferation better than harmine alone in monohormonal β cells and that selective delivery and release in β cells resulted in the same effect as a high-dose treatment. In addition, we have validated that ZnPD system does not affect insulin secretion in GSIS tests. The lack of adverse effect of zinc-chelating groups perhaps stems from the fact that the concentration of Zn(II) in the insulin granules is significantly higher (10 to 20 mM) than the concentration of chelators (20 μM) and also because the Zn(II) is being rapidly pumped into the granules by various transporters to regulate zinc homeostasis (*12*). Overall, this indicates that our ZnPD approach could be a promising method for improving the efficacy of any drug intended for modulating β cells, primarily because it increases the maximum tolerated dose by decreasing the off-target effects while it lowers the minimum efficacious dose by accumulating the drug at the site of action. We envision that this would have a wide-ranging impact on therapeutic development in β cell–targeting approaches, although further investigations regarding the mechanism of ZnPDs would be helpful to understand the reasoning behind reduced cytotoxic effects and delayed effects. In vivo testing is also needed to translate the ZnPD approach to β cells for therapeutic applications.

There are certainly some future investigations that could improve the DP. The current seeding density for cells in the DP is at 1.15×10^5 cells/mm^2, which is equivalent to 0.8 million cells per well given the current thickness and diameter of the cell disc. Although this density has greatly reduced the demand for β cells for reliable small-molecule screening, considering the scarcity and expense of primary islets and stem-cell sources, the current cell density may still pose economic burdens. In a pilot experiment, we showed that cell discs with one-third of the current diameter, or around 0.09 million cells per well, expressed similar levels of key β cell differentiation markers. Further testing could be performed to confirm the feasibility of downsizing the DP to reduce the costs associated with cell sources during medium- to high-throughput screening (HTS). Given that the DP has shown to successfully recapitulate essential cell junction markers such as CX36 and E-cad, it will also be desirable to test whether the DP is amenable to the culturing and screening of additional cell types, such as multicellular tumor spheroids and stem-cell aggregates, whose functions are highly dependent on cell-cell and cell-matrix interactions in their defined niches (*41*, *42*). Furthermore, the DP may be useful in both aiding further therapeutic discovery in the treatment of pancreatic diseases and expanding islets ex vivo for transplantation by providing an environment that mimics in vivo pancreatic conditions. Considering a rat animal model (therapeutic dosage: 6500 to 8000 IEQ/kg) (*43*), three to four cell discs with equivalent cell density in the current DP design can potentially provide enough cells for transplantation purposes.

In summary, we developed the DP, a 3D culture system that recapitulates the cellular environment and interactions of SC β cells to foster viability, differentiation, and function and used it to screen our established targeting system that selectively induces and prolongs β cell proliferation. The simple and biomimetic design of the DP makes it compatible with all standard HTS readouts, meaning it could immediately replace existing 2D experimental protocols. Because the DP reflected similar β cell behavior, expression of biological markers, and insulin secretion to 3D suspension cultures, this system will allow for the screening of critically important new β cell–targeting therapeutics in an environment more predictive of native islets. Overall, the technology presented in this study can support a more rapid and cost-effective production of a sustainable source of islets in vitro as well as potentially reduce the side effects of known small molecules for in vivo β cell expansion toward a long-term transplantation remedy for diabetes patients.

MATERIALS AND METHODS

DP fabrication

Disques (3.0-mm inner diameter) were engraved by laser cutter (Universal Laser Systems Inc., Scottsdale, AZ, USA) from 1.5-mm-thick acrylic sheets. A 1.0-μm pore size of hydrophilic PTFE membrane (Cole-Parmer, Vernon Hills, IL, USA) was attached to the bottom of a Disque using acrylic glue. The reverse side of the membrane was attached to a supporting pedestal engraved by a laser cutter. The Disques were sterilized by incubation with 70% ethanol (Sigma-Aldrich, St. Louis, MO, USA) overnight and ultraviolet (UV) radiation for 1 hour before placement into the bottom of 96-well plates (Corning, Corning, NY, USA).

Cell culture and differentiation

PP and SC β cells were provided by the Melton Lab of the Harvard Stem Cell Institute at Harvard University and cultured in 50 ml of SFs (ABLE Biott, Tokyo, Japan). For 2D and DP culture, SC β clusters were dissociated into single cells by replacing media with 1× TrypLE Express (Gibco, Thermo Fisher Scientific, Waltham, MA, USA) for incubation at 37°C for 15 min, centrifuging at 250*g* for 5 min, and washing with media twice. Dispersed SC β cells were seeded at 1.15×10^5 cells/mm^2 in the DP. To generate a cell monolayer, as a control, the cells were seeded at 1.0×10^4 cells/mm^2 in the conventional 2D plate (*44*). The DP was precoated with laminin (10 μg/ml) (Corning) and collagen IV (Corning) for 1 hour at room temperature. Seeded cells in DP were spun down at 250*g* for 5 min for reaggregation. Differentiation of SC β cells from stages 4 to 6 and media usage followed a known protocol (*22*). Experiments with SC β cells were performed with stage 6 days 10 to 15 cells unless otherwise stated. The human primary islets were provided from Prodo Laboratories (Aliso Viejo, CA, USA) and seeded into the DP as described above. Culture media for human islets were also from Prodo Laboratories [PIM(S) supplemented with PIM (ABS, G, and 3X)]. All cells were cultured at 37°C in an incubator with 5% CO_2 and 100% humidity. Human islet and donor information: purity (90%), viability (95%), health (nondiabetic), age (48 years), gender (male), ethnicity (Caucasian), cause of death (head trauma), and body mass index (30.2).

Compound treatment

Cells were seeded into the DP and incubated with their respective media as outlined in the section above and allowed to settle for 24 hours. For compound treatment (ZnPDs and multiple parent small molecules), the media were replaced with new media supplemented with prodrug at different concentrations on days 3 and 6 for a total treatment of 6 days. Cell analyses were performed after 7 days in culture. For targeting study with ZnPD4, cells were treated with ZnPD4 for an hour. For zinc pretreatment groups, after seeding, the cells were incubated with 50 μM zinc chloride (Sigma-Aldrich) for 24 hours and washed with media twice before ZnPD4 treatment. For Notch signaling inhibition, media were supplemented with DAPT (Sigma-Aldrich) at 10 μM. For the dose-cytotoxicity study, cell viability was measured by alamarBlue assay following the manufacturer's protocol (Invitrogen, Carlsbad, CA, USA).

Flow cytometry

Differentiated SC β cells in the DP and SF were dispersed into single-cell suspension by incubation in 1× TrypLE Express (Gibco) at 37°C for 15 min and then fixed with 4% paraformaldehyde (Electron Microscopy Sciences, Hatfield, PA, USA) at 4°C for 20 min and washed with phosphate-buffered saline (PBS) buffer. Cells were permeabilized with 0.1% Triton X-100 (Sigma-Aldrich) at room temperature for 30 min for EdU labeling following the manufacturer's protocol (Click-iT EdU, Invitrogen). For primary antibody labeling, cells were incubated with blocking buffer [5% donkey serum (Jackson Immunoresearch, West Grove, PA, USA) and 0.1% saponin (Sigma-Aldrich) in PBS buffer] at 4°C for 1 hour, resuspended in blocking buffer with primary antibodies, incubated at 4°C overnight, and then washed with blocking buffer twice. The following primary antibodies were used: rat monoclonal anti-Ki67 (1:500; Abcam, Cambridge, MA, USA), mouse monoclonal anti–C-peptide (1:300; R&D systems, Minneapolis, MN, USA), rabbit monoclonal anti-GCG (1:1000; Abcam, Cambridge, MA, USA), goat polyclonal anti–Pdx-1 (1:500; R&D systems), and rabbit monoclonal anti-Nkx6.1 (1:500; Abcam). For secondary antibody labeling, cells were incubated with a blocking buffer with secondary antibodies at 4°C for 45 min and washed with blocking buffer twice before analysis. The following secondary antibodies were used: 1:500 dilution: Alexa Fluor 405 goat anti-mouse immunoglobulin G (IgG) (Invitrogen), Alexa Fluor 488 goat anti-mouse IgG (Invitrogen), Alexa Fluor 488 goat anti-rat IgG (Invitrogen), and Alexa Fluor 647 donkey anti-rabbit IgG (Invitrogen). Zombie dye staining was performed before cell fixation and permeabilization at 1:500 dilution (Zombie UV, BioLegend, San Diego, CA, USA). Cells were analyzed using a BD FACSAria II flow cytometer (BD Biosciences, Franklin Lakes, NJ, USA). Analysis of the results was performed using the FlowJo (FlowJo LLC, Ashland, OR, USA) and BD FACSDiva (BD Biosciences) software.

Immunocytochemical staining

The immunofluorescent staining was performed as previously described in the "Flow cytometry" section in Materials and Methods. The additional primary antibodies for immunocytochemical staining were used: rabbit polyclonal anti-NFAT1 (1:500; Abcam, Cambridge, MA, USA), mouse monoclonal anti–E-cad (1:500; Abcam) and rabbit polyclonal anti-CX36 (1:500; Abcam). Secondary antibodies were stained using previously described antibodies noted within the flow cytometry method. Cells were then counterstained with 4′, 6-diamidino-2-phenylindole (DAPI, MilliporeSigma, Burlington, MA, USA) or Hoechst staining dye (Invitrogen). HTS imaging was performed using the Opera Phenix High Content Screening System (PerkinElmer, Waltham, MA, USA). Fluorescent and bright-field imaging were performed using the Eclipse TE2000-U (Nikon, Tokyo, Japan). Confocal imaging and *z*-stack 3D reconstruction were performed using LSM 800 with Airyscan (Zeiss, Oberkochen, Germany). Analysis was performed using ImageJ (NIH) and Adobe Photoshop (Adobe, San Jose, CA, USA) software.

Cell viability test

To determine the viability of SC β cells in the DP and SF, a LIVE/DEAD Viability and Cytotoxicity Assay Kit (alamarBlue, Invitrogen) was used according to the manufacturer's instructions.

Gene expression analysis

To analyze the gene expression of SC β cells, total RNA was isolated using the RNeasy Mini Kit (Qiagen, Chatsworth, CA, USA) from each sample ($n = 3$) according to the manufacturer's instructions. The RNA concentration was determined by measuring absorbance at 260 nm using a spectrophotometer. A reverse transcription reaction was performed with 500 ng of pure total RNA using SuperScript III First-Strand Synthesis System (Invitrogen). qRT-PCR was performed using a 7900 HT RT-PCR System (Applied Biosystems, Foster City, CA, USA). SYBR Green RT-PCR Master Mixes (Applied Biosystems) were used for the reaction. The profiles of gene expression in SC β cells were quantified for each target [human E-cad, CX36, ZnT8, Pdx-1, Nkx6.1, insulin, and glyceraldehyde 3-phosphate dehydrogenase (GAPDH), QuantiTect primary assay]. The expression level of target genes was determined by the comparative Ct method, whereby the target is normalized to the endogenous reference (GAPDH) (*45*). The relative expression of each marker in SC β cells cultured on the engineered surfaces was normalized to control.

Glucose-stimulated insulin secretion

SC β cell differentiation between 28 and 35 days was sampled in discs (1.15×10^5 cells/mm^2). Cell discs and SC β clusters were washed with PBS followed by preincubation in low (2.8 mM) glucose Krebs buffer for 2 hours to remove residual insulin. Discs and SC β clusters were then washed with PBS twice and incubated in low-glucose Krebs buffer for 30 min, and then the supernatant was collected. The discs and clusters were further washed with PBS twice and incubated in high glucose (20 mM) Krebs buffer for 30 min, and the supernatant was collected. These sequences were repeated for two additional times. Last, discs and clusters were incubated with 30 mM KCl (depolarization challenge) in PBS for 30 min, and then the supernatant was collected. These clusters were next dispersed into single cells using TrypLE Express (Gibco) for cell counting. Supernatant samples containing insulin were processed using the Human Ultrasensitive Insulin ELISA Kit (ALPCO Diagnostics, Salem, NH, USA) and normalized based on live cell numbers.

Zinc ion indication

Fluozin-3 indicator (Invitrogen) was used to detect Zn(II) in SC β cells according to the manufacturer's protocol (Invitrogen). One hour following indicator treatment to live SC β cells, confocal imaging was performed using LSM 800 with Airyscan (Zeiss). The fluorescence was also measured using a microplate reader (Infinite M200 Pro, Tecan, Maennedorf, Switzerland). Excitation and emission wavelength of 494 and 516 nm were used.

ZnPDs synthesis

For synthetic procedures, see Supplementary Materials and Methods.

Statistical analysis

All data were presented as means ± SD. For statistical evaluation, the statistical probability was calculated using ANOVA, and statistic calculations were performed using GraphPad Prism 8 software (GraphPad Software, San Diego, CA, USA). The statistical significance of the data was determined at 95% ($P < 0.05$), 99% ($P < 0.01$), and 99.9% ($P < 0.001$) confidence intervals.

SUPPLEMENTARY MATERIALS

Supplementary material for this article is available at http://advances.sciencemag.org/cgi/content/full/6/47/eabc3207/DC1

REFERENCES AND NOTES

1. A. V. Matveyenko, P. C. Butler, Relationship between β-cell mass and diabetes onset. *Diabetes Obes. Metab.* **10**, 23–31 (2008).
2. J. J. Meier, T. G. K. Breuer, R. C. Bonadonna, A. Tannapfel, W. Uhl, W. E. Schmidt, H. Schrader, Pancreatic diabetes manifests when beta cell area declines by approximately 65% in humans. *Diabetologia* **55**, 1346–1354 (2012).
3. E. A. Ryan, B. W. Paty, P. A. Senior, D. Bigam, E. Alfadhli, N. M. Kneteman, J. R. Lakey, A. M. J. Shapiro, Five-year follow-up after clinical islet transplantation. *Diabetes* **54**, 2060–2069 (2005).
4. N. Lumelsky, O. Blondel, P. Laeng, I. Velasco, R. Ravin, R. McKay, Differentiation of embryonic stem cells to insulin-secreting structures similar to pancreatic islets. *Science* **292**, 1389–1394 (2001).
5. B. Soria, E. Roche, G. Berná, T. León-Quinto, J. A. Reig, F. Martin, Insulin-secreting cells derived from embryonic stem cells normalize glycemia in streptozotocin-induced diabetic mice. *Diabetes* **49**, 157–162 (2000).
6. D. Zhang, W. Jiang, M. Liu, X. Sui, X. Yin, S. Chen, Y. Shi, H. Deng, Highly efficient differentiation of human ES cells and iPS cells into mature pancreatic insulin-producing cells. *Cell Res.* **19**, 429–438 (2009).
7. H. Zulewski, E. J. Abraham, M. J. Gerlach, P. B. Daniel, W. Moritz, B. Müller, M. Vallejo, M. K. Thomas, J. F. Habener, Multipotential nestin-positive stem cells isolated from adult pancreatic islets differentiate ex vivo into pancreatic endocrine, exocrine, and hepatic phenotypes. *Diabetes* **50**, 521–533 (2001).
8. J. Jiménez, L. Riverón-Negrete, F. Abdullaev, J. Espinosa-Aguirre, R. Rodríguez-Arnaiz, Cytotoxicity of the β-carboline alkaloids harmine and harmaline in human cell assays in vitro. *Exp. Toxicol. Pathol.* **60**, 381–389 (2008).
9. L. Egefjord, A. B. Petersen, A. M. Bak, J. Rungby, Zinc, alpha cells and glucagon secretion. *Curr. Diabetes Rev.* **6**, 52–57 (2010).
10. A. Solomou, G. Meur, E. Bellomo, D. J. Hodson, A. Tomas, S. Migrenne Li, E. Philippe, P. L. Herrera, C. Magnan, G. A. Rutter, The zinc transporter Slc30a8/ZnT8 is required in a subpopulation of pancreatic α-cells for hypoglycemia-induced glucagon secretion. *J. Biol. Chem.* **290**, 21432–21442 (2015).
11. K. Lemaire, F. Chimienti, F. Schuit, Zinc transporters and their role in the pancreatic β-cell. *J. Diabetes Investig.* **3**, 202–211 (2012).
12. Y. V. Li, Zinc and insulin in pancreatic beta-cells. *Endocrine* **45**, 178–189 (2014).
13. K. Ramachandran, S. J. Williams, H.-H. Huang, L. Novikova, L. Stehno-Bittel, Engineering islets for improved performance by optimized reaggregation in a micromold. *Tissue Eng. Part A* **19**, 604–612 (2012).
14. H.-C. Chang, C.-H. Lin, D. Juang, H.-W. Wu, C.-Y. Lee, C. Chen, C.-H. Hsu, Multilayer architecture microfluidic network array for combinatorial drug testing on 3D-cultured cells. *Biofabrication* **11**, 035024 (2019).
15. K. Yang, S. Han, Y. Shin, E. Ko, J. Kim, K. I. Park, S. Chung, S. W. Cho, A microfluidic array for quantitative analysis of human neural stem cell self-renewal and differentiation in three-dimensional hypoxic microenvironment. *Biomaterials* **34**, 6607–6614 (2013).
16. J. Amin, K. Ramachandran, S. J. Williams, A. Lee, L. Novikova, L. Stehno-Bittel, A simple, reliable method for high-throughput screening for diabetes drugs using 3D β-cell spheroids. *J. Pharmacol. Toxicol. Methods* **82**, 83–89 (2016).
17. P. Wang, J.-C. Alvarez-Perez, D. P. Felsenfeld, H. Liu, S. Sivendran, A. Bender, A. Kumar, R. Sanchez, D. K. Scott, A. Garcia-Ocana, A. F. Stewart, A high-throughput chemical screen reveals that harmine-mediated inhibition of DYRK1A increases human pancreatic beta cell replication. *Nat. Med.* **21**, 383–388 (2015).
18. J. C. Stendahl, D. B. Kaufman, S. I. Stupp, Extracellular matrix in pancreatic islets: Relevance to scaffold design and transplantation. *Cell Transplant.* **18**, 1–12 (2009).
19. K. I. Aamodt, A. C. Powers, Signals in the pancreatic islet microenvironment influence β-cell proliferation. *Diabetes Obes. Metab.* **19** (Suppl 1), 124–136 (2017).
20. M. Kragl, E. Lammert, in *The Islets of Langerhans,* M. S. Islam, Ed. (Springer Netherlands, Dordrecht, 2010).
21. M. Lee, K. Yang, Y. H. Hwang, Y. Byun, D. Y. Lee, S.-W. Cho, H. Lee, Spheroform: Therapeutic spheroid-forming nanotextured surfaces inspired by desert beetle *Physosterna cribripes*. *Adv. Healthc. Mater.* **4**, 511–515 (2015).
22. F. W. Pagliuca, J. R. Millman, M. Gürtler, M. Segel, A. Van Dervort, J. H. Ryu, Q. P. Peterson, D. Greiner, D. A. Melton, Generation of functional human pancreatic β cells in vitro. *Cell* **159**, 428–439 (2014).
23. K. Polonsky, B. Frank, W. Pugh, A. Addis, T. Karrison, P. Meier, H. Tager, A. Rubenstein, The limitations to and valid use of C-peptide as a marker of the secretion of insulin. *Diabetes* **35**, 379–386 (1986).
24. P. J. Carolan, D. A. Melton, New findings in pancreatic and intestinal endocrine development to advance regenerative medicine. *Curr. Opin. Endocrinol. Diabetes Obes.* **20**, 1–7 (2013).
25. X.-Y. Li, W.-J. Zhai, C.-B. Teng, Notch signaling in pancreatic development. *Int. J. Mol. Sci.* **17**, 48 (2016).
26. L. C. Murtaugh, B. Z. Stanger, K. M. Kwan, D. A. Melton, Notch signaling controls multiple steps of pancreatic differentiation. *Proc. Natl. Acad. Sci. U.S.A.* **100**, 14920–14925 (2003).
27. P. A. Seymour, K. K. Freude, M. N. Tran, E. E. Mayes, J. Jensen, R. Kist, G. Scherer, M. Sander, SOX9 is required for maintenance of the pancreatic progenitor cell pool. *Proc. Natl. Acad. Sci. U.S.A.* **104**, 1865–1870 (2007).
28. H. Song, Y. Zhang, Regulation of pancreatic stellate cell activation by Notch3. *BMC Cancer* **18**, 36 (2018).
29. X.-F. Zhang, R.-q. Sun, Y.-f. Jia, Q. Chen, R.-F. Tu, K.-k. Li, X.-D. Zhang, R.-L. Du, R.-h. Cao, Synthesis and mechanisms of action of novel harmine derivatives as potential antitumor agents. *Sci. Rep.* **6**, 33204 (2016).
30. X. Yang, W. Wang, J.-J. Qin, M.-H. Wang, H. Sharma, J. K. Buolamwini, H. Wang, R. Zhang, JKA97, a novel benzylidene analog of harmine, exerts anti-cancer effects by inducing G1 arrest, apoptosis, and p53-independent up-regulation of p21. *PLOS ONE* **7**, e34303 (2012).
31. K. Kumar, P. Wang, R. Sanchez, E. A. Swartz, A. F. Stewart, R. J. DeVita, Development of kinase-selective, harmine-based DYRK1A inhibitors that induce pancreatic human β-cell proliferation. *J. Med. Chem.* **61**, 7687–7699 (2018).
32. J. Shirakawa, R. N. Kulkarni, Novel factors modulating human β-cell proliferation. *Diabetes Obes. Metab.* **18** (Suppl 1), 71–77 (2016).
33. Y. J. Wang, M. L. Golson, J. Schug, D. Traum, C. Liu, K. Vivek, C. Dorrell, A. Naji, A. C. Powers, K.-M. Chang, M. Grompe, K. H. Kaestner, Single-cell mass cytometry analysis of the human endocrine pancreas. *Cell Metab.* **24**, 616–626 (2016).

34. M. Lee, B. Maji, D. Manna, S. Kahraman, R. M. Elgamal, J. Small, P. Kokkonda, A. Vetere, J. M. Goldberg, S. J. Lippard, R. N. Kulkarni, B. K. Wagner, A. Choudhary, Native zinc catalyzes selective and traceless release of small molecules in β-cells. *J. Am. Chem. Soc.* **142**, 6477–6482 (2020).
35. W. Chyan, D. Y. Zhang, S. J. Lippard, R. J. Radford, Reaction-based fluorescent sensor for investigating mobile Zn^{2+} in mitochondria of healthy versus cancerous prostate cells. *Proc. Natl. Acad. Sci. U.S.A.* **111**, 143–148 (2014).
36. A. Veres, A. L. Faust, H. L. Bushnell, E. N. Engquist, J. H.-R. Kenty, G. Harb, Y.-C. Poh, E. Sintov, M. Gürtler, F. W. Pagliuca, Q. P. Peterson, D. A. Melton, Charting cellular identity during human in vitro β-cell differentiation. *Nature* **569**, 368–373 (2019).
37. G. Kim, K.-H. Shin, E.-K. Pae, Zinc up-regulates insulin secretion from β cell-like cells derived from stem cells from human exfoliated deciduous Tooth (SHED). *Int. J. Mol. Sci.* **17**, 2092 (2016).
38. K. G. Slepchenko, N. A. Daniels, A. Guo, Y. V. Li, Autocrine effect of Zn^{2+} on the glucose-stimulated insulin secretion. *Endocrine* **50**, 110–122 (2015).
39. K. Rüben, A. Wurzlbauer, A. Walte, W. Sippl, F. Bracher, W. Becker, Selectivity profiling and biological activity of novel β-carbolines as potent and selective DYRK1 kinase inhibitors. *PLOS ONE* **10**, e0132453 (2015).
40. O. Maguire, K. M. Tornatore, K. L. O'Loughlin, R. C. Venuto, H. Minderman, Nuclear translocation of nuclear factor of activated T cells (NFAT) as a quantitative pharmacodynamic parameter for tacrolimus. *Cytometry A* **83**, 1096–1104 (2013).
41. J. Friedrich, C. Seidel, R. Ebner, L. A. Kunz-Schughart, Spheroid-based drug screen: Considerations and practical approach. *Nat. Protoc.* **4**, 309–324 (2009).
42. P. R. Baraniak, T. C. McDevitt, Scaffold-free culture of mesenchymal stem cell spheroids in suspension preserves multilineage potential. *Cell Tissue Res.* **347**, 701–711 (2012).
43. S.-H. Lee, E. Hao, A. Y. Savinov, I. Geron, A. Y. Strongin, P. Itkin-Ansari, Human β-cell precursors mature into functional insulin-producing cells in an immunoisolation device: Implications for diabetes cell therapies. *Transplantation* **87**, 983–991 (2009).
44. A. Chowdhury, V. P. Satagopam, L. Manukyan, K. A. Artemenko, Y. M. E. Fung, R. Schneider, J. Bergquist, P. Bergsten, Signaling in insulin-secreting MIN6 pseudoislets and monolayer cells. *J. Proteome Res.* **12**, 5954–5962 (2013).
45. K. Yang, S. J. Yu, J. S. Lee, H.-R. Lee, G.-E. Chang, J. Seo, T. Lee, E. Cheong, S. G. Im, S.-W. Cho, Electroconductive nanoscale topography for enhanced neuronal differentiation and electrophysiological maturation of human neural stem cells. *Nanoscale* **9**, 18737–18752 (2017).
46. R. K. P. Benninger, W. S. Head, M. Zhang, L. S. Satin, D. W. Piston, Gap junctions and other mechanisms of cell-cell communication regulate basal insulin secretion in the pancreatic islet. *J. Physiol.* **589**, 5453–5466 (2011).
47. A. Calabrese, D. Caton, P. Meda, Differentiating the effects of Cx36 and E-cadherin for proper insulin secretion of MIN6 cells. *Exp. Cell Res.* **294**, 379–391 (2004).
48. M. A. Ravier, M. Güldenagel, A. Charollais, A. Gjinovci, D. Caille, G. Söhl, C. B. Wollheim, K. Willecke, J.-C. Henquin, P. Meda, Loss of connexin36 channels alters β-cell coupling, islet synchronization of glucose-induced Ca^{2+} and insulin oscillations, and basal insulin release. *Diabetes* **54**, 1798–1807 (2005).
49. J. Kim, I. K. Shim, D. G. Hwang, Y. N. Lee, M. Kim, H. Kim, S.-W. Kim, S. Lee, S. C. Kim, D.-W. Cho, J. Jang, 3D cell printing of islet-laden pancreatic tissue-derived extracellular matrix bioink constructs for enhancing pancreatic functions. *J. Mater. Chem. B* **7**, 1773–1781 (2019).
50. A. Chowdhury, O. Dyachok, A. Tengholm, S. Sandler, P. Bergsten, Functional differences between aggregated and dispersed insulin-producing cells. *Diabetologia* **56**, 1557–1568 (2013).
51. Z. Li, H. Sun, J. Zhang, H. Zhang, F. Meng, Z. Cui, Development of in vitro 3D TissueFlex® islet model for diabetic drug efficacy testing. *PLOS ONE* **8**, e72612 (2013).
52. F. Chimienti, S. Devergnas, F. Pattou, F. Schuit, R. Garcia-Cuenca, B. Vandewalle, J. Kerr-Conte, L. Van Lommel, D. Grunwald, A. Favier, M. Seve, In vivo expression and functional characterization of the zinc transporter ZnT8 in glucose-induced insulin secretion. *J. Cell Sci.* **119**, 4199–4206 (2006).
53. Y. Ichihara, R. Utoh, M. Yamada, T. Shimizu, Y. Uchigata, Size effect of engineered islets prepared using microfabricated wells on islet cell function and arrangement. *Heliyon* **2**, e00129 (2016).
54. O. G. Kelly, M. Y. Chan, L. A. Martinson, K. Kadoya, T. M. Ostertag, K. G. Ross, M. Richardson, M. K. Carpenter, K. A. D'Amour, E. Kroon, M. Moorman, E. E. Baetge, A. G. Bang, Cell-surface markers for the isolation of pancreatic cell types derived from human embryonic stem cells. *Nat. Biotechnol.* **29**, 750–756 (2011).
55. J. B. Gurdon, A. Mitchell, D. Mahony, Direct and continuous assessment by cells of their position in a morphogen gradient. *Nature* **376**, 520–521 (1995).
56. J. B. Gurdon, P. Harger, A. Mitchell, P. Lemaire, Activin signalling and response to a morphogen gradient. *Nature* **371**, 487–492 (1994).
57. C. A. Fraker, S. Alvarez, P. Papadopoulos, J. Giraldo, W. Gu, C. Ricordi, L. Inverardi, J. Domínguez-Bendala, Enhanced oxygenation promotes β-cell differentiation in vitro. *Stem Cells* **25**, 3155–3164 (2007).
58. A. Lindström, J. Carlsson, Penetration and binding of epidermal growth factor-dextran conjugates in spheroids of human glioma origin. *Cancer Biother.* **8**, 145–158 (1993).
59. M. A. Dewit, E. R. Gillies, A cascade biodegradable polymer based on alternating cyclization and elimination reactions. *J. Am. Chem. Soc.* **131**, 18327–18334 (2009).
60. D. Song, J. M. Lim, S. Cho, S. J. Park, J. Cho, D. Kang, S. G. Rhee, Y. You, W. Nam, A fluorescence turn-on H_2O_2 probe exhibits lysosome-localized fluorescence signals. *Chem. Commun. (Camb.)* **48**, 5449–5451 (2012).
61. Y. Lee, G. Y. Park, H. R. Lucas, P. L. Vajda, K. Kamaraj, M. A. Vance, A. E. Milligan, J. S. Woertink, M. A. Siegler, A. A. Narducci Sarjeant, L. N. Zakharov, A. L. Rheingold, E. I. Solomon, K. D. Karlin, Copper(I)/O_2 chemistry with imidazole containing tripodal tetradentate ligands leading to μ-1,2-peroxo-dicopper(II) species. *Inorg. Chem.* **48**, 11297–11309 (2009).

Acknowledgments: We thank A. R. Gannon, B. D. Pope, A. L. Glieberman, K. K. Parker, J. Small, J. Choi for the helpful discussions contributed to this study and E. N. Engquist, Y. Yu, K. Biles, J. Zhang for providing us with SC β cells from the Melton Lab cell foundry. **Funding:** This work was supported by the Burroughs Wellcome Fund (Career Award at the Scientific Interface) and NIH (UC4DK116255 and R01 DK113597) to A.C. This work was also supported by NIH (Human Islet Research Network-Consortium on Human Islet Biomimetics, HIRN-CHIB) (UC4DK104165) to J.M.K. and D.A.M. D.A.M. was also supported from the Harvard Stem Cell Institute. **Author contributions:** K.Y., P.A.J., and J.M.K. conducted the Disque Platform design and validation. M.L. and A.C. conducted the ZnPD design and validation was conducted by K.Y., M.L., A.C., and J.M.K. K.Y., M.L., P.A.J., S.S.L., A.Z., J.X., V.S., J.L.Y.W., and L.V. conducted the experiments and/or data analysis. K.Y., M.L., S.S.L., A.Z., A.C., and J.M.K. wrote the paper. P.A.J., E.A.L., R.P., Y.L., B.K.W., and D.A.M. provided input and reviewed the paper. All authors reviewed and edited the manuscript. **Competing interests:** AC is an inventor on an international patent that claims inventions related to targeted delivery to β cells filed by the Broad Institute (no. PCT/US2018/028660, filed 20 April 2018). J.M.K. is an inventor on a patent related to this work filed by Brigham and Women's Hospital, and licensed to Mesoblast (no. US8,956,863 B2, filed 15 October 2010). J.M.K. and A.C. are inventors on a patent application related to this work filed by Brigham and Women's Hospital and the Broad Institute (no. 63/039,863, filed 16 June 2020). J.M.K. has been a paid consultant and or equity holder for companies including Stempeutics, Sanofi, Celltex, LifeVaultBio, Camden Partners, Stemgent, Biogen, Pancryos, Element Biosciences, Frequency Therapeutics, and Mesoblast. J.M.K. holds equity in Frequency Therapeutics, a company that has licensed IP generated by J.M.K. that may benefit financially if the IP is further validated. The interests of J.M.K. were reviewed and are subject to a management plan overseen by his institutions in accordance with its conflict of interest policies. D.A.M. holds equity in Vertex Pharmaceuticals and serves as a consultant at the same. The authors declare no other competing interests. **Data materials and availability:** All data needed to evaluate the conclusions in the paper are present in the paper and/or the Supplementary Materials. Additional data related to this paper may be requested from the authors.

Submitted 23 April 2020
Accepted 7 October 2020
Published 18 November 2020
10.1126/sciadv.abc3207

Citation: K. Yang, M. Lee, P. A. Jones, S. S. Liu, A. Zhou, J. Xu, V. Sreekanth, J. L. Y. Wu, L. Vo, E. A. Lee, R. Pop, Y. Lee, B. K. Wagner, D. A. Melton, A. Choudhary, J. M. Karp, A 3D culture platform enables development of zinc-binding prodrugs for targeted proliferation of β cells. *Sci. Adv.* **6**, eabc3207 (2020).